Biogeosciences Discuss., 12, 5169–5199, 2015
www.biogeosciences-discuss.net/12/5169/2015/
doi:10.5194/bgd-12-5169-2015

Biogeosciences
Discussions
Open Access

Links between surface productivity and deep ocean particle flux at the Porcupine Abyssal Plain (PAP) sustained observatory

H. Frigstad[1,*], S. A. Henson[2], S. E. Hartman[2], A. M. Omar[1,3], E. Jeansson[1], H. Cole[4], C. Pebody[2], and R. S. Lampitt[2]

[1]Uni Research Climate, Allégaten 55, 5007 Bergen, Norway
[2]National Oceanography Centre, Waterfront Campus, European Way, Southampton SO14 3ZH, UK
[3]Geophysical Institute, University of Bergen, Allégaten 79, 5007 Bergen, Norway
[4]Ocean and Earth Science, University of Southampton Waterfront Campus, European Way, Southampton, SO14 3ZH, UK
[*]now at: the Norwegian Environment Agency, Grensesvingen 7, 0661 Oslo, Norway

Received: 9 March 2015 – Accepted: 10 March 2015 – Published: 1 April 2015

Correspondence to: H. Frigstad (helene.frigstad@miljodir.no)

Published by Copernicus Publications on behalf of the European Geosciences Union.

Abstract

In this study we present hydrography, biogeochemistry and sediment trap observations between 2003 and 2012 at Porcupine Abyssal Plain (PAP) sustained observatory in the northeast Atlantic. The time series is valuable as it allows for investigation of the link between surface productivity and deep ocean carbon flux. The region is a perennial sink for CO_2, with an average uptake of around 1.5 mmol m^{-2} d^{-1}. The average monthly drawdowns of inorganic carbon and nitrogen were used to quantify the net community production (NCP) and new production, respectively. Seasonal NCP and new production were found to be 4.57 ± 0.27 mol C m^{-2} and 0.37 ± 0.14 mol N m^{-2}. The Redfield ratio was high (12), and the production calculated from carbon was higher than production calculated from nitrogen, which is indicative of carbon overconsumption. The export ratio and transfer efficiency were 16 and 4 %, respectively, and the site thereby showed high flux attenuation. Particle tracking was used to examine the source region of material in the sediment trap, and there was large variation in source regions, both between and within years. There were higher correlations between surface productivity and export flux when using the particle-tracking approach, than by comparing with the mean productivity in a 100 km box around the PAP site. However, the differences in correlation coefficients were not significant, and a longer time series is needed to draw conclusions on applying particle tracking in sediment trap analyses.

1 Introduction

The Porcupine Abyssal Plain (PAP) sustained observatory is situated in the northeast Atlantic Ocean (49° N, 16.5° W) in a water depth of 4800 m. It is at or near the boundary between the sub-polar and sub-tropical gyres of the North Atlantic (Henson et al., 2009). A time series of particle flux measurements at 3000 m depth are available back to the early 1990's (Lampitt et al., 2010), and since 2003 there has also been a multidisciplinary full depth mooring with instruments at approximately 30 m depth

BGD
12, 5169–5199, 2015

recording hydrography, nitrate (NO_3), partial pressure of CO_2 (pCO_2) and Chlorophyll *a* (Chl *a*) (Hartman et al., 2012). The simultaneous observations of surface and deep ocean biogeochemistry make this time series ideal to study linkages between surface ocean productivity and deep ocean particle flux.

The pathway by which a small fraction (< 1 %; Martin et al., 1987) of the carbon fixed by photosynthesis in the sunlit upper ocean is exported to great depths, thereby constituting a sink for atmospheric CO_2, is referred to as the biological carbon pump. Carbon sinking to the deep ocean is sequestered on long time scales (100s to 1000s of years), and therefore quantifying the biological carbon pump is key in understanding the global carbon cycle (Falkowski et al., 1998; Sabine et al., 2004). The PAP time series allows an investigation of the factors controlling the flux of carbon. These factors are currently not fully understood, so it is therefore difficult to predict how they will respond to climate change (e.g. Passow and Carlson, 2012).

Primary production in the surface ocean can be measured by several techniques (broadly separated into vitro incubations or changes in bulk properties; Platt et al. (1989), however, from the perspective of the oceanic carbon cycle the most important rate is the net community production (NCP). NCP is the net primary production (NPP) minus heterotrophic respiration, and represents the sum of the particulate and dissolved organic carbon available for export or utilization by higher trophic levels. NCP is traditionally measured by bottle O_2 incubations (Gaarder and Gran, 1927), but has also been estimated from oxygen or carbon budgets, ^{234}Thorium, sediment traps and O_2/Ar ratios. The multitude of methods and difficulty in comparing techniques has lead to a poor understanding of NCP rates in many regions of the ocean (Quay et al., 2010). In many studies, the steady-state NCP is equated with the export flux at the base of the euphotic zone (Platt et al., 1989; Lee, 2001; Long et al., 2011; Nevison et al., 2012), based on the rationale that NCP is the organic material available for export out of the mixed layer. However, it is not directly comparable to the most common definition of export flux (i.e. the downward flux of POC at a nominal depth) as NCP represents a bulk measurement integrated over the mixed layer and long time scales (and also includes

BGD
12, 5169–5199, 2015

the contribution of DOC to export). The export ratio (ie. Dugdale and Goering, 1967) is used to quantify the proportion of the organic material produced that is exported below the euphotic zone, and is often calculated as the flux of POC at 100 m divided by the NPP (Henson et al., 2012). Global estimates of the export ratio range from 10 % (Henson et al., 2011) to 40 % (Eppley and Peterson, 1979), and is well correlated with temperature, and thereby also latitude (Laws et al., 2000).

New production (Dugdale and Goering, 1967) is the production supported by the input of new nitrogen into the euphotic zone through upwelling and horizontal mixing, but also by processes such as atmospheric deposition and nitrogen fixation (Sarmiento and Gruber, 2006; Gruber, 2008). On an annual basis, assuming the system is in steady state, export production is considered equivalent to new production (Eppley and Peterson, 1979).

From a climate change perspective, the long-term (> 100 years) removal of carbon from the atmosphere is important to quantify, which is often defined as the flux of carbon below 1000 m (Lampitt et al., 2008), known as the sequestration flux. The sequestration flux is smaller than the export flux out of the euphotic zone or mixed layer, and is ~ 6–25 % of the new production based on sediment trap data (Berelson, 2001; Francois et al., 2002). This large reduction in carbon flux with increasing depth is caused by intensive remineralization of organic material as it sinks through the mesopelagic zone, which is often referred to as flux attenuation (Martin et al., 1987; Steinberg et al., 2008). The ratio of deep POC flux to export flux (POC flux at 2000 m/POC flux at 100 m), is known as the transfer efficiency and describes the efficiency of the biological pump (Francois et al., 2002; De La Rocha and Passow, 2012; Henson et al., 2012).

In this study we present a time series of surface ocean measurements and particle trap data from the PAP observatory station from 2003 to 2012. Our aim is twofold; firstly, we will quantify NCP and new production from the average monthly drawdown of dissolved inorganic carbon (DIC) and NO_3, respectively. This allows us to compare these two estimates of surface productivity, and derive export ratios by comparison with satellite NPP estimates and published values of shallow POC flux at the PAP

BGD
12, 5169–5199, 2015

observatory. Secondly, we will investigate the link between the production at the surface and particle flux at 3000 m depth, both by investigating the transfer efficiency and by examining the source location of exported material using particle-tracking techniques.

2 Data and methods

2.1 PAP surface mooring

Hydrographical and biogeochemical parameters were measured using data from instruments at a nominal 30 m depth on a full depth mooring at the PAP observatory (49° N, 16.5° W). The surface mooring was first deployed in July 2003, and more information about the time series can be found in Hartman et al. (2012). Due to problems with damage to the mooring and/or failure of sensors, there is no or little data between 2005 and 2010, however, after May 2010 there is good temporal coverage for all biogeochemical parameters. The data from 2003–2005 have previously been published in Kortzinger et al. (2008) and Hartman et al. (2010) and the sensors and calibrations used during these deployments will not be discussed further here. The sensors used after 2005 are described in Table 1 in Hartman et al. (2012), and are Seabird MicroCAT for temperature and salinity, Satlantic ISUS for NO_3 (+ nitrite), Wetlabs (FLNTUSB) for Chl *a* and PRO-OCEANUS for pCO_2. The NO_3, Chl *a* and pCO_2 data have all been quality controlled and calibrated against CTD data on cruises to the PAP observatory at deployment and/or recovery of the mooring, while this has not always been achieved for temperature and salinity.

2.2 Sediment trap

The sediment trap mooring at the PAP observatory was deployed in the depth range 3000 to 3200 m, which is around 1800 m above the seabed. The methodology is described in Lampitt et al. (2010), but briefly a Parflux sediment trap was used with mouth area 0.5 m^2, prefilled with hypersaline buffered formalin, following the JGOFS protocols.

BGD
12, 5169–5199, 2015

The collection period varied between 2 and 8 weeks depending on the time of year and anticipated flux. All fluxes are temporally and spatially integrated, and given in either $mL\,m^{-2}\,d^{-1}$ (volume flux) or $mg\,m^{-2}\,d^{-1}$ (dry weight and Particulate Organic Carbon (POC)).

2.3 Ancillary data and calculated parameters

To interpret and expand on the data from the PAP observatory, the following parameters were used from external data sources (see Table 1): temperature and salinity profiles from Argo floats, atmospheric CO_2 concentration, sea level barometric pressure (SLP), wind speed at 10 m height and satellite derived net primary production (NPP).

Temperature and salinity profiles were extracted from the global fields for the PAP observatory (49° N, 16.5° W), made available by the Coriolis project (http://www.coriolis.eu.org). The gridded fields use temperature and salinity profiles collected by Argo floats, XBTs, CTD/XCTDs and moorings, and the irregularly sampled data are gridded onto a regularly spaced grid by the statistical objective analysis method (Gaillard et al., 2009). The North Atlantic is the region most frequently sampled by Argo floats and has good coverage in both time and space (Gaillard et al., 2009). Here we use monthly averaged temperature and salinity fields for 2002–2009 (delayed mode data), however, after 2010 only near real-time data were available, which has undergone less rigorous quality control than the delayed mode data. In the calculation of carbon parameters (below) the Argo float temperature and salinity at 30 m were used, because of data gaps in the temperature and salinity data from the PAP sensor (referred to as Argo temperature and salinity in text and Figs. 1 and 2) and the lack of consistent calibration with CTD data. Density profiles were calculated using the recently updated standard for seawater properties (TEOS-10; www.teos-10.org). The mixed layer depth (MLD) was calculated from density profiles using the same global gridded fields used for the temperature and salinity data at 30 m. The depth of the mixed layer was defined by a density difference of $0.03\,kg\,m^{-3}$ from the density at a reference depth (in this case 10 m to avoid diurnal changes in temperature and salinity at the surface). We

BGD
12, 5169–5199, 2015

followed the algorithm developed by Holte and Talley (2009), which incorporates linear interpolation to estimate the exact depth at which the density difference is crossed.

The atmospheric CO_2 concentration measurements were obtained from the observatory closest to the PAP observatory, the Mace Head land station in Ireland (53.33° N, 9.90° W) from the Cooperative Atmospheric Data Integration Projects (GLOBALVIEW-CO2, 2012). There were no measurements available after 2010, and so the annual averaged growth rate in atmospheric CO_2 for marine sites from the NOAA ESRL data for 2011 (1.69 $\mu mol\,mol^{-1}$) and 2012 (2.59 $\mu mol\,mol^{-1}$) was added to the seasonal cycle in CO_2 concentrations at the Mace Head station for 2010 (http://www.esrl.noaa.gov/gmd/ccgg/trends/global.html). The atmospheric pCO_2 was calculated using the Mace Head station CO_2 measurements at barometric pressure (6 hourly Sea Level Pressure; Table 1) and equilibrium water vapour pressure (from Argo temperature and salinity at 30 m; Table 1).

The air–sea CO_2 flux (in $mmol\,m^{-2}\,d^{-1}$) was calculated from the air–sea pCO_2 difference, Argo temperature and salinity (30 m) and wind speed at 10 m height, using the following equation:

$$F_{CO_2} = k \times K_0 \times (pCO_{2sea} - pCO_{2air}) \quad (1)$$

where k is the transfer coefficient based on the wind speed-dependent formulation of Nightingale et al. (2000) scaled to the temperature-dependent Schmidt number according to Wanninkhof (1992), K_0 is the CO_2 solubility at in situ temperature and salinity (Argo temperature and salinity at 30 m) after Weiss (1974), while pCO_{2sea} and pCO_{2air} are the CO_2 partial pressures of seawater and air, respectively.

The alkalinity (Alk) was calculated from Argo temperature and salinity (30 m), following the relationship for the North Atlantic developed by Lee et al. (2006). The dissolved inorganic carbon (DIC) was calculated from Alk and measured pCO_2 using the "seacarb" package (Lavigne and Gattuso, 2011), developed for R (R Development Core Team, 2012), using Argo temperature and salinity (30 m) and nutrient concentrations set to zero. The chosen constants were Lueker et al. (2000) for K_1 and K_2, Perez

BGD
12, 5169–5199, 2015

and Fraga (1987) for K_f and the Dickson (1990) constant for K_s, as recommended by Dickson et al. (2007).

The seasonal drawdown of DIC and NO_3 were used to quantify the NCP and new production, respectively. The gaps in the PAP time series did not allow for examination of the seasonal drawdown on an annual basis (expect for the year of 2004, as published by Kortzinger et al., 2008). However, for each month of the year data from at least two to four different years were available. Therefore, NCP and new production were estimated two to four times for each of the months January–November (an explanation for December to be followed shortly). This allowed the quantification of the average seasonal NCP and new production and variability (expressed as one SD) from the PAP time series. The monthly changes in Eqs. (3) and (4) (below) were computed in a circular manner i.e. the change in the 12th month is the difference January minus December. Data from three different years were available for both of these months, but they coincided only for 2004. Therefore, NCP and new production in December could be estimated only once (based on the 2004 data) and, thus, the variability could not be estimated for this month. An additional source of variability in NCP and new production estimates come from measurement uncertainty, which propagates into calculated values. However, the variability associated with measurement uncertainty is negligible compared to the natural variability. For instance, the measurement uncertainty for the NO_3 sensor given by the manufacturer (Satlantic ISUS V3 sensor) was $\pm 2\,\mu mol\,kg^{-1}$. This gives a propagated probable error in the NO_{3MLD} estimates of $< 0.001\,mol\,N\,m^{-2}$ (calculated from the square root of the sum of squared errors), which is considered negligible compared to the uncertainty associated with monthly variation (see Fig. 3). Similarly, using $\pm 3\,\mu mol\,kg^{-1}$ as the uncertainty in DIC and AlK values (e.g.,Millero, 1995) does not include errors by using Alk calculated from salinity) gives a probable propagated error of $< 0.05\,mol\,C\,m^{-2}$, which is small compared to the uncertainty from monthly variation in Fig. 3.

The monthly changes in DIC concentrations (ΔDIC_{obs}) can be attributed to changes caused by air–sea gas exchange (ΔDIC_{gas}), physical mixing processes (ΔDIC_{mix}) and

BGD
12, 5169–5199, 2015

biological production (ΔDIC_{BP}). The monthly (ΔDIC_{gas}) (in $\mu mol\,kg^{-1}$) can be estimated from the air–sea CO_2 flux (F_{CO_2}) and MLD by the following formulation:

$$\Delta DIC_{gas} = \frac{F_{CO_2}}{MLD} \times \frac{365}{12} \tag{2}$$

The contribution of ΔDIC_{mix} was assumed negligible, and ΔDIC_{BP} was assumed to be largely determined by NCP (excluding the effect of calcification). The monthly NCP integrated over the MLD (NCP_{MLD} in $mol\,C\,m^{-2}$) was calculated from the monthly changes in DIC corrected for the effects of air–sea gas exchange ($\Delta DIC^{GasCorr}$):

$$NCP_{MLD} = \left(\Delta DIC^{GasCorr}_{m+1} - \Delta DIC^{GasCorr}_{m}\right) \times \frac{(MLD_{m+1} + MLD_m)}{2} \tag{3}$$

where $\Delta DIC^{GasCorr}_{m+1} - \Delta DIC^{GasCorr}_{m}$ is the difference in $\Delta DIC^{GasCorr}\Delta DIC^{GasCorr}$ between two consecutive months (m and $m+1$) and the last term gives the average MLD of the two months. Positive values of NCP_{MLD} represents net autotrophy (i.e. the months where the biological drawdown of DIC exceeds the DIC released by heterotrophic processes), and the seasonal NCP_{MLD} can then be calculated as the sum of months with a positive NCP.

The same rationale can be applied to the monthly changes in NO_3 concentrations (ΔNO_3), naturally without having to consider the effect of air–sea exchange. The monthly MLD-integrated NO_3 changes (ΔNO_3 in $mol\,N\,m^{-2}$) were calculated as:

$$NO_{3MLD} = (\Delta NO_{3m+1} - \Delta NO_{3m}) \times \frac{(MLD_{m+1} + MLD_m)}{2} \tag{4}$$

Summing up the months with a net drawdown in NO_3 gives the seasonal new production.

Net primary production (NPP) was estimated from satellite data using the Vertically Generalised Production Model (Behrenfeld and Falkowski, 1997), which requires inputs

BGD
12, 5169–5199, 2015

of chlorophyll concentration, sea surface temperature and photosynthetically available radiation data, here taken from NASA's MODIS Aqua satellite (reprocessing R2012.0). Data were downloaded from the Ocean Productivity website (see Table 1).

2.4 Particle tracking and cross-correlations

In addition to estimating the surface origin of particles sinking to the sediment trap using a simple 100 km box around the PAP observatory, we also used modelled velocity fields to determine the likely source region. The velocity field (u and v components) was taken from the NEMO model (Madec, 2008) run at NOC at 5 day, 1/4° resolution for the period 2002–2011. The model has 75 depth levels increasing in thickness with depth, ranging from 1 m near surface to 200 at 6000 m depth. All particles reaching the PAP sediment trap at 3000 m depth are assumed to have a sinking speed of 100 m d^{-1} and particles are tracked backwards in time in 3 dimensions by linear interpolation of the gridded velocity field to the local position of the particle, until they reach the surface (30 days after release).

The cross-correlation between the sediment trap data and either NPP in a 100 km box around the PAP observatory or in source locations identified by particle tracking, were calculated using the ccf function in R (R Development Core Team, 2012). The cross-correlations were performed on monthly anomalies (monthly climatology – observed monthly value), to avoid possible inflation of p values due to auto-correlation. To test for significant differences between the correlation coefficients the Fisher r-to-z transformation was used (two-tailed test, with two dependent correlations sharing one variable), from the R library "Psych" (Fisher, 1915; Revelle, 2012).

3 Results

Time series data from 2003 to 2012 from the PAP surface mooring and sediment trap are shown in Fig. 1. The temperature and salinity (both PAP sensors and Argo

BGD
12, 5169–5199, 2015

30 m) varied in the range 12–18 °C and 35.4–35.8, respectively. The mixed layer depths (MLD) were fairly consistent between years, although the winter mixed layer only extended down to ∼ 100 m in 2010. There was a pronounced seasonal drawdown in pCO_2 (similarly for DIC), with summer values as low as 300 µatm during August 2004 and typical winter values between 360–380 µatm. Corresponding seasonal trends were seen for NO_3, with a winter maximum of 10 µmol kg^{-1} in March 2004 and values close to detection limit during summer. The strongest bloom was observed in June 2011 with Chl *a* concentrations between 3 and 5 µg L^{-1}, with higher than typical summer values of around 2 µg L^{-1}. The air–sea CO_2 flux was negative (i.e. oceanic uptake of CO_2) throughout the time period, with an average uptake of around 1.5 mmol m^{-2} d^{-1}. There were three years with unusually high sediment fluxes, with short bursts of high flux during summer in 2004, 2009 and 2012.

The monthly climatology (or average seasonal cycle) for temperature showed a seasonal warming of around 5 °C, with very good overlap between the temperatures measured by the PAP sensor and the Argo floats at 30 m (see monthly climatologies in Fig. 2). There was little seasonal variation in salinity, although the Argo float data is generally around 0.05 lower than the salinity measured by the sensors at the PAP observatory. The summer MLD was around 30 m (usually between May and October), and mixing extended down to 250 m depth in winter. The pCO_2 decreased by around 30 µatm from winter values to the summer minimum in August (reduction of around 35 µmol kg^{-1} for DIC), while NO_3 decreased by around 5 µmol kg^{-1} to the summer minimum typically found in September. There was a gradual build-up of Chl *a* from February, with highest values typically found between May and July with large SD reflecting the high interannual variability in Fig. 1. There was no clear seasonal signal in air–sea CO_2 flux, with high variability throughout the year. The sediment fluxes also had high interannual variability, however, the highest volume flux was typically found in June, while an autumn peak was often found for dry weight and POC in September or October.

BGD
12, 5169–5199, 2015

The monthly MLD-integrated NO_3 changes (NO_{3MLD}) were positive from February to August (Fig. 3), which means that during these months there was a net decrease in NO_3 concentrations in the mixed layer caused by biological drawdown. Conversely, there were negative NO_{3MLD} from September to February, meaning that during these months the NO_3 concentrations increased due to remineralization and entrainment of new nutrients through winter mixing. This corresponds to a MLD-integrated seasonal new production (from February to August, see Sect. 2.3 for calculation) of $0.37 \pm 0.14\,\mathrm{mol\,N\,m^{-2}}$. Note that all uncertainties given for production estimates in this work are due to interannual variability, as explained in Sect. 2.3. The monthly MLD-integrated changes in NCP (NCP_{MLD}) showed the same seasonal trend, with a positive NCP_{MLD} (i.e. decrease in DIC concentrations) from February to July. In addition, there was a much higher NCP_{MLD} in March compared to the other spring/summer months. The MLD-integrated seasonal NCP (from February to July) was $4.57 \pm 0.27\,\mathrm{mol\,C\,m^{-2}}$.

Tracking of the particles arriving at the sediment trap at 3000 m at the PAP observatory (see Sect. 2.4), revealed that the source locations of particles could vary substantially between years, and also on an annual time scale (Fig. 4). The satellite NPP in these source regions also varied markedly, and the highest NPP of around $2500\,\mathrm{mg\,C\,m^{-2}\,d^{-1}}$ was found in 2009.

There was a high cross-correlation between the seasonal anomalies of NPP in source locations identified by the particle tracking and the volume flux in the sediment trap (+0.62; Fig. 5) at lag = 0 months. The corresponding cross-correlation for NPP averaged over a 100 km box around the PAP observatory and volume flux was considerably lower (+0.48; Fig. 5), however the difference between the two cross-correlations was not significant (Fisher transformation, $n = 111$, $z = 1.58$, $p = 0.11$). The correlation coefficients between either dry weight or POC and the two different NPP estimates were lower, and similarly showed no significant difference between either using the NPP identified by particle tracking or a 100 km box. The highest cross-correlations between NPP and dry weight was found at lag = −1 month (i.e. dry weight lagged NPP by one month), while it was at lag = −3 months for NPP and POC. We also tested the

BGD
12, 5169–5199, 2015

cross-correlations using the NPP at the exact latitude and longitude of the PAP observatory (49° N, 16° W) and extending the box to 200 km around the observatory, but there were no significant differences in cross-correlations using these instead of the mean of a 100 km box around the PAP observatory as above (results not shown).

4 Discussion

4.1 Estimates of surface productivity

The seasonal cycles of carbon (pCO_2/DIC) and NO_3 at the PAP observatory are characteristic of highly productive sub-polar regions, where cooling, convection and remineralization cause a winter maximum, while drawdown from biological production during spring and summer causes a minimum during late summer (Takahashi et al., 2002). This is true also for pCO_2, because the decreasing effect of production is stronger than the opposing effect of warming. The same seasonal effects are seen in the MLD integrated changes in NO_3 and DIC concentrations used to calculate new production and NCP (i.e. Fig. 3). There were positive monthly changes in NO_{3MLD} and NCP_{MLD} during spring/summer, due to decreasing concentrations related to biological production within a shallowing or fairly stable mixed layer. During winter the combined effects of cooling, deep mixing and remineralization caused negative NO_{3MLD} and NCP_{MLD} (i.e. increasing NO_3 and DIC concentrations).

The MLD-integrated seasonal NCP (from February to July) was $4.57 \pm 0.27\,\mathrm{mol\,C\,m^{-2}}$, which is comparable to, but lower than, the NCP calculated for the PAP observatory by Kortzinger et al. (2008) for 2004 of $6.4 \pm 1.1\,\mathrm{mol\,C\,m^{-2}}$ from March to early August. This is natural given that Kortzinger et al. (2008) integrated over a much deeper fixed mixed layer (238 m) from March until mid May, while here we used the mean MLD between consecutive months. As can be seen in Fig. 2, the MLD shallows rapidly from around 250 m in March to 50 m in May, and we believe using the actual depth of the mixed layer gives a more realistic estimate of NCP during this period of

BGD
12, 5169–5199, 2015

rapid stratification. Consistent with Kortzinger et al. (2008), we find that the strongest NCP occurs before the onset of shallow stratification in summer, with a NCP maximum in March. The MLD-integrated seasonal new production (from February to August) was $0.37 \pm 0.14\,\mathrm{mol\,N\,m^{-2}}$. This is within the range of new production estimates, using different approaches, from 0.23–1.1 $\mathrm{mol\,N\,m^{-2}}$ from the northeast Atlantic Ocean and Icelandic Sea (Fernández I et al., 2005; Hartman et al., 2010; Jeansson et al., 2015).

Converting the new production in terms of nitrogen to carbon units using the Redfield ratio of 6.6 (Redfield, 1958), gives a value of $2.5\,\mathrm{mol\,C\,m^{-2}}$, which is substantially smaller than the NCP calculated from DIC changes. However, there is not necessarily any basis for assuming that new production and NCP should be equal, even in a steady state system (cf. Laws, 1991). This would imply that carbon is assimilated and recycled by heterotrophs (as respiration is included in NCP) in the same ratio as nitrogen is assimilated by autotrophs during new production, which need not be the case (i.e. variable stoichiometry, see review by Sterner and Elser, 2002). The fact that the production calculated from carbon is higher than the production calculated from nitrogen, is referred to as carbon overconsumption (Toggweiler, 1993), and has been demonstrated repeatedly in the North Atlantic (Sambrotto et al., 1993; Kortzinger et al., 2001; Koeve, 2006). It has also been shown specifically for the PAP observatory (Kortzinger et al., 2008; Painter et al., 2010). The seasonal C : N ratio for the PAP observatory from this study (i.e. NCP/new production) would be ≈ 12, which is greatly exceeding the Redfield ratio, although within the range of C : N ratios previously found in this region (Koeve, 2006; Kortzinger et al., 2008; Painter et al., 2010).

In regions where N_2 fixation is not thought to be an important factor, the C overconsumption must be sustained by preferential remineralization of nutrients, either in slowly sinking detritus (Sambrotto et al., 1993; Thomas et al., 1999; Kortzinger et al., 2001) or a build up of C-rich (and N-poor) DOM in the euphotic zone (Williams, 1995; Kahler and Koeve, 2001: Falck and Anderson, 2005). Additionally transparent exopolymer particles (TEP; Alldredge et al., 1993), which have been shown to have high C : N ratios (Engel and Passow, 2001) could represent a route for the C overconsumed in the euphotic

BGD
12, 5169–5199, 2015

zone to reach the deep ocean (Koeve, 2005). The regenerated nutrients can fuel additional production in the euphotic zone, and consequently estimates of new production based on nitrate might underestimate production rates (Thomas et al., 1999).

The degree to which the C overconsumed in the surface waters reaches the deep ocean, and thus is sequestered on long time scales is important, because it represents a potential negative feedback on atmospheric CO_2. Compilation of existing data sets have shown an increasing C : N of sinking material due to preferential remineralization of nutrients (Schneider et al., 2003), and the potential feedback of a depth dependent C : N ratio can influence atmospheric CO_2 concentrations by about 20 parts per million (Schneider et al., 2004). However, the deep ocean remineralization ratio of C : N has been shown to be close to the Redfield ratio (Anderson and Sarmiento, 1994), and if the C overconsumption is mainly during summer (Koeve, 2004; Jiang et al., 2013) and remineralized above the depth of the winter mixed layer, it could be questioned whether the "extra-Redfield" C is sequestered in the deeper ocean, and can therefore influence the oceanic C-budget on longer time scales (Koeve, 2006). However, the deep ocean remineralization rates of Anderson and Sarmiento (1994) did not include the Atlantic Ocean, because this basin was too complex for the chosen method. A study on the remineralization ratios in the North Atlantic Ocean specifically showed higher than Redfield C : nutrient ratios in the remineralized material in the deeper waters, and thereby a higher C drawdown by the biological carbon pump than would be expected from applying Redfield ratios in the formation of organic matter (Thomas, 2002).

Comparing our estimates of NCP and new production with satellite-derived estimates of NPP could shed some light on the balance between autotrophy and heterotrophy in this region. Summing the average monthly satellite NPP in a 100 km box around the PAP observatory from the period March to July gives $\sim 10\,\mathrm{mol\,C\,m^{-2}}$, which is about double the estimated seasonal NCP at the PAP observatory. This would imply approximately equal contributions from NCP and heterotrophic respiration to NPP (as NCP = NPP – heterotrophic respiration). However, it is questionable whether estimates of surface productivity (as given in this study) can be directly compared with satellite

BGD
12, 5169–5199, 2015

NPP. The NCP and new production are estimated based on changes in bulk properties over fairly long timescales, and are integrated over the mixed layer (assuming that the measurements made at ~ 30 m depth are representative for the entire mixed layer). While the satellite-derived estimates of NPP are often based on shorter timescales and different depth profiles, and therefore the two estimates of surface productivity can involve fundamentally different timescales (cf. Platt et al., 1989). An additional complicating factor is that NCP theoretically includes all the carbon contained in organic material, both the particulate and dissolved fraction, while the satellite NPP would only include the autotrophic component of POC.

The export flux of POC around the PAP observatory has been quantified in several studies using different techniques (see overview in Fig. 4 in Riley et al. (2012)). The average POC flux in the upper 170 m obtained from PELAGRA drifting sediment trap deployments for short periods of time (3–5 days) between 2003 and 2005 was 72 mg C m^{-2} d^{-1} (Lampitt et al., 2008). During a cruise in August 2009 the flux was found to be 84 and 146 mg C m^{-2} d^{-1} at 50 m, using PELAGRA and a marine snow catcher, respectively (Riley et al., 2012). Using the ^{234}Th technique the flux of POC at 100 m in the vicinity of the PAP observatory was determined to be 64 and 207 mg C m^{-2} d^{-1} (Lampitt et al., 2008; Thomalla et al., 2008). The export ratio describes the efficiency of nutrient utilization in the euphotic zone, and is often calculated as the POC flux at the base of the euphotic zone or a fixed depth (typically 100 m), divided by the NPP (De La Rocha and Passow, 2012; Henson et al., 2012). Using an average of the above values for POC flux out of the surface layer of 115 mg C m^{-2} d^{-1} and the March–July average NPP in the 100 km box around the PAP observatory of 772 mg C m^{-2} d^{-1} gives an export ratio of 0.15. This is identical to the estimate by Lampitt et al. (2008) for the PAP observatory during post-bloom conditions from 2003–2005, and consistent with the estimate by Henson et al. (2011) of between 10 and 30 % for temperate and sub-polar waters, respectively.

BGD
12, 5169–5199, 2015

4.2 Links between surface production and deep ocean flux of POC

Using particle tracking to identify the source location of material arriving in the sediment trap at 3000 m at the PAP observatory showed that the particles could originate up to 140 km away (in 2007; Fig. 4). There was large variation in the source location of particles between years, depending on the prevailing current conditions in the given year. There was also large variation within individual years, but the satellite NPP generally increased during spring and decreased during autumn along the trajectory of the particles reflecting the seasonal cycle. The highest NPP was found in 2009 ($> 2000\,\mathrm{mg\,C\,m^{-2}\,d^{-1}}$), which corresponds to very high fluxes in both volume flux and dry weight in the sediment trap at the PAP observatory (Fig. 1). Interestingly, there was not a strong bloom at the PAP observatory according to the in situ Chl *a* observations at 30 m depth (sensor data available from May to late July; Fig. 1), while the satellite NPP showed high correlations with the volume flux and dry weight in the sediment trap. The correlations were highest between the NPP in source locations as identified by particle tracking, compared to the mean NPP in a fixed 100 km box around the PAP observatory. However, the differences in correlation coefficients were not statistically different, and more observations ($n = 111$ in present analysis) would be needed to determine if using a particle tracking approach when examining the origin of particles in sediment traps indeed gives higher correlations.

The transfer efficiency is used to describe the efficiency of the biological carbon pump, and is a useful metric to describe the long-term removal of carbon (> 100 years) from the atmosphere (cf. De La Rocha and Passow, 2012). Using the same average POC flux of the surface layer (0–170 m) as in the calculation of the export flux above and the average flux between March and July of POC at 3000 m from the sediment trap at the PAP observatory ($5.1\,\mathrm{mg\,C\,m^{-2}\,d^{-1}}$), the transfer efficiency was calculated to be 4 %. This corresponds well with the transfer efficiency between 5 and 10 % found for the 50° N region by Henson et al. (2012). The fairly high export ratio (15 %) and low transfer efficiency (4 %) fits the description of the general trends in high latitude

BGD
12, 5169–5199, 2015

ecosystems in the above-cited study well. This dichotomy in efficiencies implies that although a large proportion of the primary production is exported below the euphotic zone, this material is relatively labile and is efficiently remineralized in the mesopelagic zone, so that only a very small fraction of the exported organic matter reaches the deep ocean and is stored on long time scales.

The PAP observatory is currently at or close to the boundary between the sub-polar and sub-tropical gyres of the North Atlantic, and will likely transition into more sub-tropical conditions as the gyres expand over the next century (Sarmiento et al., 2004). It has been shown that seasonably variable areas, like the sub-polar region, export a higher fraction of labile material than sub-tropical regions (Lutz et al., 2007), which could imply that the current export regime of the PAP observatory is likely to change as a result of climate change.

5 Conclusions

The PAP observatory is characterized by strong interannual variability in hydrography, biogeochemistry, and especially sediment fluxes. The seasonal cycles of carbon and nitrogen show a winter maximum and summer minimum, characteristic of highly productive sub-polar regions. The MLD-integrated seasonal NCP (from February to July) was $4.57 \pm 0.27\,\mathrm{mol\,C\,m^{-2}}$, which is consistent, with but slightly lower than the estimate by Kortzinger et al. (2008) for 2004. The MLD-integrated seasonal new production (from February to August) was $0.37 \pm 0.14\,\mathrm{mol\,N\,m^{-2}}$, which gives a Redfield ratio (NCP/new production) of 12, corroborating other reports of carbon overconsumption for the North Atlantic and the PAP observatory specifically (Sambrotto et al., 1993; Kortzinger et al., 2001, 2008; Koeve, 2006; Painter et al., 2010).

The export ratio was 15 %, while the transfer efficiency was 4 %, which is typical of high latitude ecosystems where, although a large proportion of the primary production is exported out of the euphotic zone, this material is relatively labile and therefore remineralized before it reaches the deep ocean. It is hypothesized that the export regime at

BGD
12, 5169–5199, 2015

the PAP observatory could change with climate change, as the region will probably transition into more sub-tropical conditions over the next century (Sarmiento et al., 2004; Lutz et al., 2007).

Using particle tracking to identify the source regions of material reaching the sediment trap at the PAP observatory, revealed higher correlations between NPP in the identified source regions and export flux than other methods. However, more observations are needed to establish if a particle-tracking approach indeed gives added value in sediment trap analyses.

Acknowledgements. We would like to acknowledge the various ship crew, engineers and scientists involved in preparation, deployment and recovery of the PAP sustained observatory moorings, especially Jon Campbell and Mark Hartman. We wish to thank Maureen Pagnani, Athanos Gkritzalis-Papadopoulos, Zong-Pei Jiang and Andres Cianca for compilation, quality control and calibration of PAP data. Mooring data and support for this research was provided by the European research projects ANIMATE (Atlantic Network of Interdisciplinary Moorings and Time-Series for Europe), MERSEA (Marine Environment and Security for the European Sea), EUROCEANS (European Network of Excellence for Ocean Ecosystems Analysis) and EuroSITES grant agreement EU 202955. The work was also supported through the Natural Environment Research Council (NERC), UK, project Oceans 2025 and National Capability. H. Frigstad was supported by EU FP7, through projects MEECE (212085), EURO-BASIN (264933) and GreenSeas (265294).

References

Alldredge, A. L., Passow, U., and Logan, B. E.: The abundance and significance of a class of large, transparent organic particles in the ocean, Deep-Sea Res. Pt. I, 40, 1131–1140, 1993.

Anderson, L. A. and Sarmiento, J. L.: Redfield ratios of remineralization determined by nutrient data-analysis, Global Biogeochem. Cy., 8, 65–80, 1994.

Behrenfeld, M. J. and Falkowski, P. G.: Photosynthetic rates derived from satellite-based chlorophyll concentration, Limnol. Oceanogr., 42, 1–20, 1997.

Berelson, W. M.: The flux of partuculate organic carbon into the ocean interior: a comparison of four U.S. JGOFS regional studies, Oceanography, 14, 59–67, 2001.

De La Rocha, C. L. and Passow, U. (Eds): The Biological Pump, vol. 6., Elsevier, Oxford, 2012.
Dickson, A. G.: Standard potential of the reaction – Agcl(S) + 1/2h-2(G) = Ag(S) + Hcl(Aq) and the standard acidity constant of the ion Hso4 – in synthetic sea-water from 273.15-K to 318.15-K, J. Chem. Thermodyn., 22, 113–127, 1990.
Dickson, A. G., Sabine, C. L., and Chrsitian, J. R.: Guide to Best Practices for Ocean, CO_2 Measurements., PICES Special Publication, Book 3, 2007.
Dugdale, R. C. and Goering, J. J.: Uptake of new and regenerated forms of nitrogen in primary productivity, Limnol. Oceanogr., 12, 196–206, 1967.
Engel, A. and Passow, U.: Carbon and nitrogen content of transparent exopolymer particles (TEP) in relation to their Alcian Blue adsorption, Mar. Ecol.-Prog. Ser., 219, 1–10, 2001.
Eppley, R. W. and Peterson, B. J.: Particulate organic-matter flux and planktonic new production in the deep ocean, Nature, 282, 677–680, 1979.
Falck, E. and Anderson, L. G.: The dynamics of the carbon cycle in the surface water of the Norwegian Sea, Mar. Chem., 94, 43–53, 2005.
Falkowski, P. G., Barber, R. T., and Smetacek, V.: Biogeochemical controls and feedbacks on ocean primary production, Science, 281, 200–206, 1998.
Fernández, I. C., Raimbault, P., Garcia, N., Rimmelin, P., and Caniaux, G.: An estimation of annual new production and carbon fluxes in the northeast Atlantic Ocean during 2001, J. Geophys. Res.-Oceans, 110, C07S13, doi:10.1029/2004JC002616, 2005.
Fisher, R. A.: Frequency distribution of the values of the correlation coefficient in samples of an indefinitely large population, Biometrika, 10, 507–521, 1915.
Francois, R., Honjo, S., Krishfield, R., and Manganini, S.: Factors controlling the flux of organic carbon to the bathypelagic zone of the ocean, Global Biogeochem. Cy., 16, 34-1–34-20, 2002.
Gaarder, T. and Gran, H. H.: Investigation of the production of phytoplankton in the Oslo Fjord, Rap. Proces., 42, 1–48, 1927.
Gaillard, F., Autret, E., Thierry, V., Galaup, P., Coatanoan, C., and Loubrieu, T.: Quality control of large argo datasets, J. Atmos. Ocean. Tech., 26, 337–351, 2009.
GLOBALVIEW-CO2: Cooperative Atmospheric Data Integration Project – Carbon Dioxide, NOAA ESRL, Boulder, Colorado, available at: http://www.esrl.noaa.gov/gmd/ccgg/globalview/ (last access: 15 May 2013), 2012.

BGD
12, 5169–5199, 2015

Gruber, N.: The marine nitrogen cycle: overview and challenges, in: Nitrogen in the Marine Environment, edited by: Capone, D. G., Bronk, D. A., Mulholland, M. R., and Carpenter, E. J., Book 2, Elsevier, Amsterdam, 1–50, 2008.

Hartman, S. E., Larkin, K. E., Lampitt, R. S., Lankhorst, M., and Hydes, D. J.: Seasonal and inter-annual biogeochemical variations in the Porcupine Abyssal Plain 2003–2005 associated with winter mixing and surface circulation, Deep-Sea Res. Pt. II., 57, 1303–1312, 2010.

Hartman, S. E., Lampitt, R. S., Larkin, K. E., Pagnani, M., Campbell, J., Gkritzalis, T., Jiang, Z. P., Pebody, C. A., Ruhl, H. A., Gooday, A. J., Bett, B. J., Billett, D. S. M., Provost, P., McLachlan, R., Turton, J. D., and Lankester, S.: The Porcupine Abyssal Plain fixed-point sustained observatory (PAP-SO): variations and trends from the Northeast Atlantic fixed-point time-series, Ices J. Mar. Sci., 69, 776–783, 2012.

Henson, S. A., Dunne, J. P., and Sarmiento, J. L.: Decadal variability in North Atlantic phytoplankton blooms, J. Geophys. Res.-Oceans, 114, C04013, doi:10.1029/2008JC005139, 2009.

Henson, S. A., Sanders, R., Madsen, E., Morris, P. J., Le Moigne, F., and Quartly, G. D.: A reduced estimate of the strength of the ocean's biological carbon pump, Geophys. Res. Lett., 38, L04606, doi:10.1029/2011GL046735, 2011.

Henson, S. A., Sanders, R., and Madsen, E.: Global patterns in efficiency of particulate organic carbon export and transfer to the deep ocean, Global Biogeochem. Cy., 26, GB1028, doi:10.1029/2011GB004099, 2012.

Holte, J. and Talley, L.: A new algorithm for finding mixed layer depths with applications to argo data and subantarctic mode water formation, J. Atmos. Ocean. Tech., 26, 1920–1939, 2009.

Jeansson, E., Bellerby, R. G. J., Skjelvan, I., Frigstad, H., Ólafsdóttir, S. R., and Olafsson, J.: Fluxes of carbon and nutrients to the Iceland Sea surface layer and inferred primary productivity and stoichiometry, Biogeosciences, 12, 875–885, doi:10.5194/bg-12-875-2015, 2015.

Jiang, Z.-P., Hydes, D. J., Tyrrell, T., Hartman, S. E., Hartman, M. C., Dumousseaud, C., Padin, X. A., Skjelvan, I., and González-Pola, C.: Key controls on the seasonal and interannual variations of the carbonate system and air–sea CO_2 flux in the Northeast Atlantic (Bay of Biscay), J. Geophys. Res.-Oceans, 118, 785–800, 2013.

Kahler, P. and Koeve, W.: Marine dissolved organic matter: can its C : N ratio explain carbon overconsumption? Deep-Sea Res. Pt. I, 48, 49–62, 2001.

Koeve, W.: Spring bloom carbon to nitrogen ratio of net community production in the temperate N. Atlantic, Deep-Sea Res. Pt. I, 51, 1579–1600, 2004.

BGD
12, 5169–5199, 2015

Koeve, W.: Magnitude of excess carbon sequestration into the deep ocean and the possible role of TEP, Mar. Ecol.-Prog. Ser., 291, 53–64, 2005.
Koeve, W.: C : N stoichiometry of the biological pump in the North Atlantic: constraints from climatological data, Global Biogeochem. Cy., 20, GB3018, doi:10.1029/2004GB002407, 2006.
Kortzinger, A., Koeve, W., Kahler, P., and Mintrop, L.: C : N ratios in the mixed layer during the productive season in the northeast Atlantic Ocean, Deep-Sea Res. Pt. I, 48, 661–688, 2001.
Kortzinger, A., Send, U., Lampitt, R. S., Hartman, S., Wallace, D. W. R., Karstensen, J., Villagarcia, M. G., Llinas, O., and DeGrandpre, M. D.: The seasonal pCO_2 cycle at 49° N/16.5° W in the northeastern Atlantic Ocean and what it tells us about biological productivity, J. Geophys. Res.-Oceans, 113, C04020, doi:10.1029/2007JC004347, 2008.
Lampitt, R. S., Boorman, B., Brown, L., Lucas, M., Salter, I., Sanders, R., Saw, K., Seeyave, S., Thomalla, S. J., and Turnewitsch, R.: particle export from the euphotic zone: estimates using a novel drifting sediment trap, Th-234 and new production, Deep-Sea Res. Pt. I, 55, 1484–1502, 2008.
Lampitt, R. S., Salter, I., de Cuevas, B. A., Hartman, S., Larkin, K. E., and Pebody, C. A.: Long-term variability of downward particle flux in the deep northeast Atlantic: causes and trends, Deep-Sea Res. Pt. II., 57, 1346–1361, 2010.
Lavigne, H. and Gattuso, J.-P.: Seacarb: seawater carbonate chemistry with R, R package version 2.4., available at: http://CRAN.R-project.org/package=seacarb (last access: 10 May 2013), 2011.
Laws, E. A.: Photosynthetic quotients, new production and net community production in the open ocean, Deep-Sea Res., 38, 143–167, 1991.
Laws, E. A., Falkowski, P. G., Smith, W. O., Ducklow, H., and McCarthy, J. J.: Temperature effects on export production in the open ocean, Global Biogeochem. Cy., 14, 1231–1246, 2000.
Lee, K.: Global net community production estimated from the annual cycle of surface water total dissolved inorganic carbon, Limnol. Oceanogr., 46, 1287–1297, 2001.
Long, M. C., Dunbar, R. B., Tortell, P. D., Smith, W. O., Mucciarone, D. A., and DiTullio, G. R.: Vertical structure, seasonal drawdown, and net community production in the Ross Sea, Antarctica, J. Geophys. Res.-Oceans, 116, C10029, doi:10.1029/2009JC005954, 2011.
Lueker, T. J., Dickson, A. G., and Keeling, C. D.: Ocean pCO_2 calculated from dissolved inorganic carbon, alkalinity, and equations for K-1 and K-2: validation based on laboratory measurements of CO2 in gas and seawater at equilibrium, Mar. Chem., 70, 105–119, 2000.

BGD
12, 5169–5199, 2015

Lutz, M. J., Caldeira, K., Dunbar, R. B., and Behrenfeld, M. J.: Seasonal rhythms of net primary production and particulate organic carbon flux to depth describe the efficiency of biological pump in the global ocean, J. Geophys. Res.-Oceans, 112, C10011, doi:10.1029/2006JC003706., 2007.

Madec, G.: NEMO ocean engine, Note du Pole de modélisation, Institut Pierre-Simon Laplace (IPSL), France, No 27 ISSN No 1288-1619, 2008.

Martin, J. H., Knauer, G. A., Karl, D. M., and Broenkow, W. W.: Vertex – carbon cycling in the northeast Pacific, Deep-Sea Res., 34, 267–285, 1987.

Millero, F. J.: The thermodynamics of the carbonic acid system in the oceans, Geochim. Cosmochim. Ac., 59, 661–667, 1995.

Nevison, C. D., Keeling, R. F., Kahru, M., Manizza, M., Mitchell, B. G., and Cassar, N.: Estimating net community production in the Southern Ocean based on atmospheric potential oxygen and satellite ocean color data, Global Biogeochem. Cy., 26, doi:10.1029/2011gb004040, 2012.

Nightingale, P. D., Malin, G., Law, C. S., Watson, A. J., Liss, P. S., Liddicoat, M. I., Boutin, J., and Upstill-Goddard, R. C.: In situ evaluation of air–sea gas exchange parameterizations using novel conservative and volatile tracers, Global Biogeochem. Cy., 14, 373–387, 2000.

Painter, S. C., Lucas, M. I., Stinchcombe, M. C., Bibby, T. S., and Poulton, A. J.: Summertime trends in pelagic biogeochemistry at the Porcupine Abyssal Plain study site in the northeast Atlantic, Deep-Sea Res. Pt. II., 57, 1313–1323, 2010.

Passow, U. and Carlson, C. A.: The biological pump in a high CO_2 world, Mar. Ecol.-Prog. Ser., 470, 249–271, 2012.

Perez, F. F. and Fraga, F.: Association constant of fluoride and hydrogen-ions in seawater, Mar. Chem., 21, 161–168, 1987.

Platt, T., Harrison, W. G., Lewis, M. R., Li, W. K. W., Sathyendranath, S., Smith, R. E., and Vezina, A. F.: Biological production of the oceans – the case for a consensus, Mar. Ecol.-Prog. Ser., 52, 77–88, 1989.

Quay, P. D., Peacock, C., Bjorkman, K., and Karl, D. M.: Measuring primary production rates in the ocean: enigmatic results between incubation and non-incubation methods at Station ALOHA, Global Biogeochem. Cy., 24, GB3014, doi:10.1029/2009GB003665, 2010.

Redfield, A. C.: The biological control of chemical factors in the environment, Am. Sci., 46, 205–221, 1958.

BGD
12, 5169–5199, 2015

Revelle, W.: Psych: Procedures for Personality and Psychological Research Northwestern University, Evanston, available at: http://CRAN.R-project.org/package=psych (last access: 20 May 2013), 1.2.1., 2012.

Riley, J. S., Sanders, R., Marsay, C., Le Moigne, F. A. C., Achterberg, E. P., and Poulton, A. J.: The relative contribution of fast and slow sinking particles to ocean carbon export, Global Biogeochem. Cy., 26, GB1026, doi:10.1029/2011GB004085, 2012.

Sabine, C. L., Feely, R. A., Gruber, N., Key, R. M., Lee, K., Bullister, J. L., Wanninkhof, R., Wong, C. S., Wallace, D. W. R., Tilbrook, B., Millero, F. J., Peng, T. H., Kozyr, A., Ono, T., and Rios, A. F.: The oceanic sink for anthropogenic CO_2, Science, 305, 367–371, 2004.

Sambrotto, R. N., Savidge, G., Robinson, C., Boyd, P., Takahashi, T., Karl, D. M., Langdon, C., Chipman, D., Marra, J., and Codispoti, L.: Elevated consumption of carbon relative to nitrogen in the surface ocean, Nature, 363, 248–250, 1993.

Sarmiento, J. L. and Gruber, N.: Ocean Biogeochemical Dyamics, Princeton University Press, Princeton, New Jersey, USA, 2006.

Sarmiento, J. L., Slater, R., Barber, R., Bopp, L., Doney, S. C., Hirst, A. C., Kleypas, J., Matear, R., Mikolajewicz, U., Monfray, P., Soldatov, V., Spall, S. A., and Stouffer, R.: Response of ocean ecosystems to climate warming, Global Biogeochem Cy, 18, GB3003, doi:10.1029/2003GB002134, 2004.

Schneider, B., Schlitzer, R., Fischer, G., and Nothig, E. M.: Depth-dependent elemental compositions of particulate organic matter (POM) in the ocean, Global Biogeochem. Cy., 17, 1032, doi:10.1029/2002GB001871, 2003.

Schneider, B., Engel, A., and Schlitzer, R.: Effects of depth- and CO_2-dependent C : N ratios of particulate organic matter (POM) on the marine carbon cycle, Global Biogeochem. Cy., 18, GB2015, doi:10.1029/2003GB002184, 2004.

Steinberg, D. K., Cope, J. S., Wilson, S. E., and Kobari, T.: A comparison of mesopelagic mesozooplankton community structure in the subtropical and subarctic North Pacific Ocean, Deep-Sea Res. Pt. II., 55, 1615–1635, 2008.

Sterner, R. W. and Elser, J. J.: Ecological Stoichiometry: the Biology of Elements from Molecules to the Biosphere, Princeton University Press, Princeton, New Jersey, 2002.

Takahashi, T., Sutherland, S. C., Sweeney, C., Poisson, A., Metzl, N., Tilbrook, B., Bates, N., Wanninkhof, R., Feely, R. A., Sabine, C., Olafsson, J., and Nojiri, Y.: Global sea–air CO_2 flux based on climatological surface ocean pCO_2, and seasonal biological and temperature effects, Deep-Sea Res. Pt. II., 49, 1601–1622, 2002.

BGD
12, 5169–5199, 2015

Team RDC: R: a language and environment for statistical computing, R Foundation for Statistical Computing, Vienna, Austria, 2012.
Thomalla, S. J., Poulton, A. J., Sanders, R., Turnewitsch, R., Holligan, P. M., and Lucas, M. I.: Variable export fluxes and efficiencies for calcite, opal, and organic carbon in the Atlantic Ocean: a ballast effect in action? Global Biogeochem. Cy., 22, GB1010, doi:10.1029/2007GB002982, 2008.
Thomas, H.: Remineralization ratios of carbon, nutrients, and oxygen in the North Atlantic Ocean: a field databased assessment, Global Biogeochem. Cy., 16, 1051, doi:10.1029/2001GB001452, 2002.
Thomas, H., Ittekkot, V., Osterroht, C., and Schneider, B.: Preferential recycling of nutrients – the ocean's way to increase new production and to pass nutrient limitation? Limnol. Oceanogr., 44, 1999–2004, 1999.
Toggweiler, J. R.: Oceanography – carbon overconsumption, Nature, 363, 210–211, 1993.
Wanninkhof, R.: Relationship between wind-speed and gas-exchange over the ocean, J. Geophys. Res.-Oceans, 97, 7373–7382, 1992.
Weiss, R. F.: Carbon dioxide in water and seawater: the solubility of a non-ideal gas, Mar. Chem., 2, 203–215, 1974.
Williams, P. J. L.: Evidence for the seasonal accumulation of carbon-rich dissolved organic material, its scale in comparison with changes in particulate material and the consequential effect on net C/N assimilation ratios, Mar. Chem., 51, 17–29, 1995.

BGD
12, 5169–5199, 2015

Table 1. Overview of ancillary data.

Parameter	Source
ARGO Temperature and salinity	Temperature and salinity fields: 1° by 1°, monthly temporal resolution. Depth in profiles had resolution of 5 m between 10 and 100 and 10 m between 100 and 800 m. Available through Coriolis project; http://www.coriolis.eu.org/
Atmospheric CO_2	Mace Head land station in Ireland (53.33N 9.90W) from the Cooperative Atmospheric Data Integration Projects (GLOBALVIEW-CO2, 2012); http://www.esrl.noaa.gov/gmd/ccgg/globalview/co2/co2_download.html
Sea Level Pressure (SLP)	FNMOC 1° by 1°, 6 hourly; http://www.pfeg.noaa.gov/products/las/docs/fnmoc_1deg_mon.nc.html
Wind speed	FNMOC 1° by 1°, 6 hourly at 10 m height; http://www.pfeg.noaa.gov/products/las/docs/windaves.nc.html
Net primary production (NPP)	Vertically Generalised Production Model; http://www.science.oregonstate.edu/ocean.productivity/index.php

BGD
12, 5169–5199, 2015

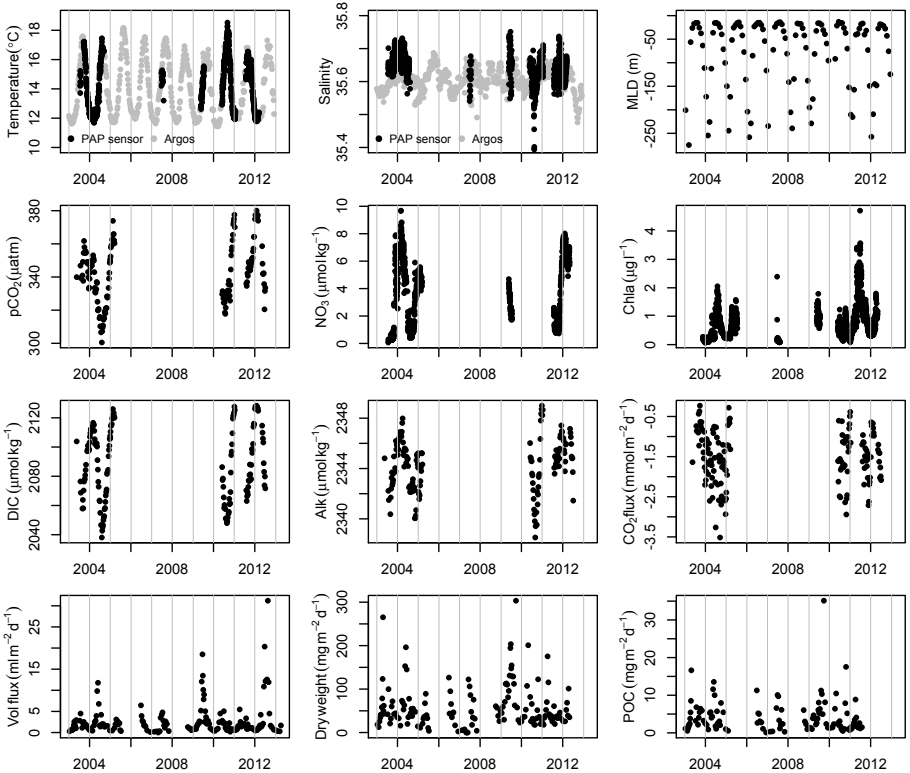

Figure 1. Time series of available data from PAP surface mooring and sediment trap. Temperature and salinity calculated from the Argo float data (grey dots in first two panels) is also shown, along with derived mixed layer depth estimates. Negative CO_2 flux values indicate flux from the atmosphere to the ocean.

BGD
12, 5169–5199, 2015

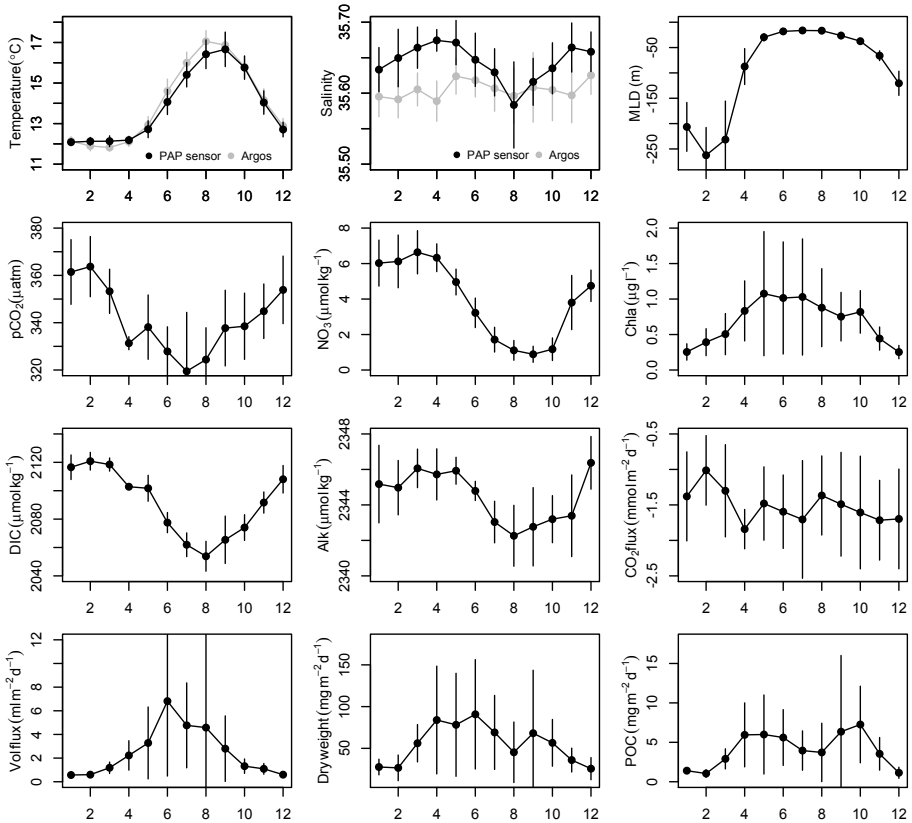

Figure 2. Monthly climatology with ±1 SD (vertical bars) of available data from PAP surface mooring (30 m) and sediment trap. Temperature and salinity calculated from the Argo float data (grey dots in first two panels) is also shown, along with derived mixed layer depth estimates.

BGD
12, 5169–5199, 2015

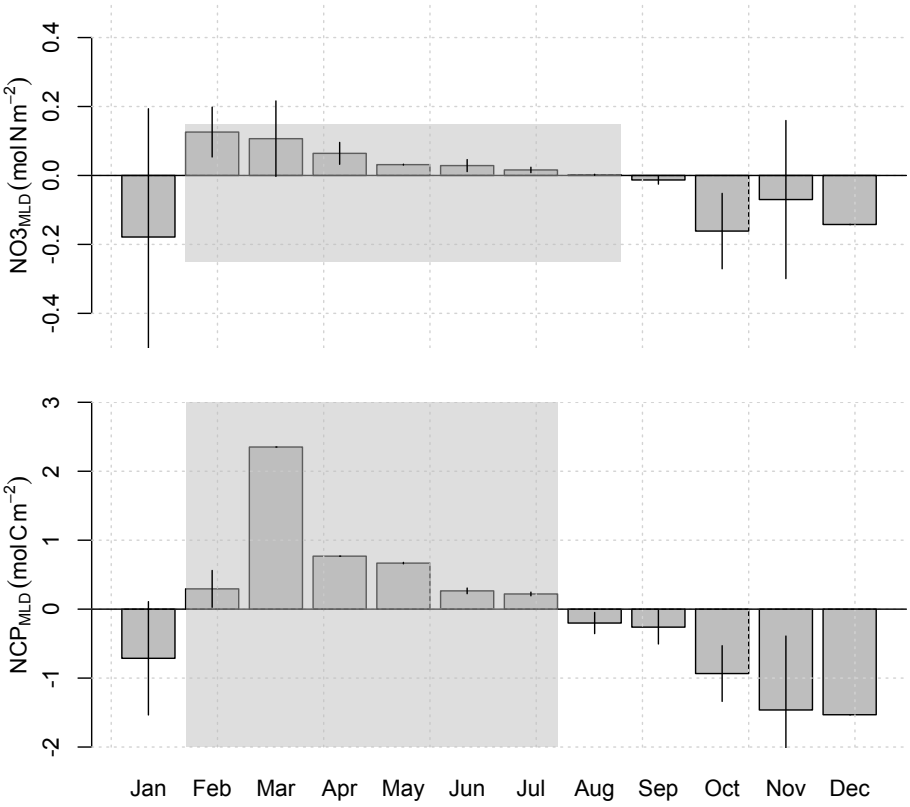

Figure 3. Monthly changes in MLD integrated NO_3 (top) and NCP (bottom). The shaded grey area indicates the months over which the seasonal new production (NO_{3MLD}: $0.37 \pm 0.14\,mol\,N\,m^{-2}$) and seasonal NCP ($NCP_{MLD}$: $4.57 \pm 0.27\,mol\,C\,m^{-2}$) were calculated. See Sect. 2.3 for calculations.

BGD
12, 5169–5199, 2015

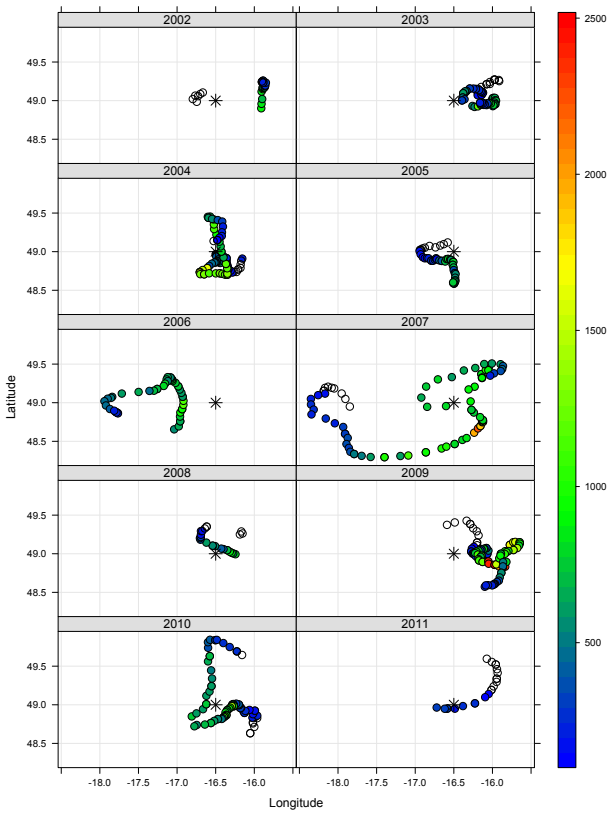

Figure 4. Satellite NPP (mg C m^{-2} d^{-1}) in the source regions for the sediment trap as identified by particle tracking. The star shows the position of the PAP mooring and unfilled circles indicate that no NPP estimate was available from satellite data (most often during January and February).

BGD
12, 5169–5199, 2015

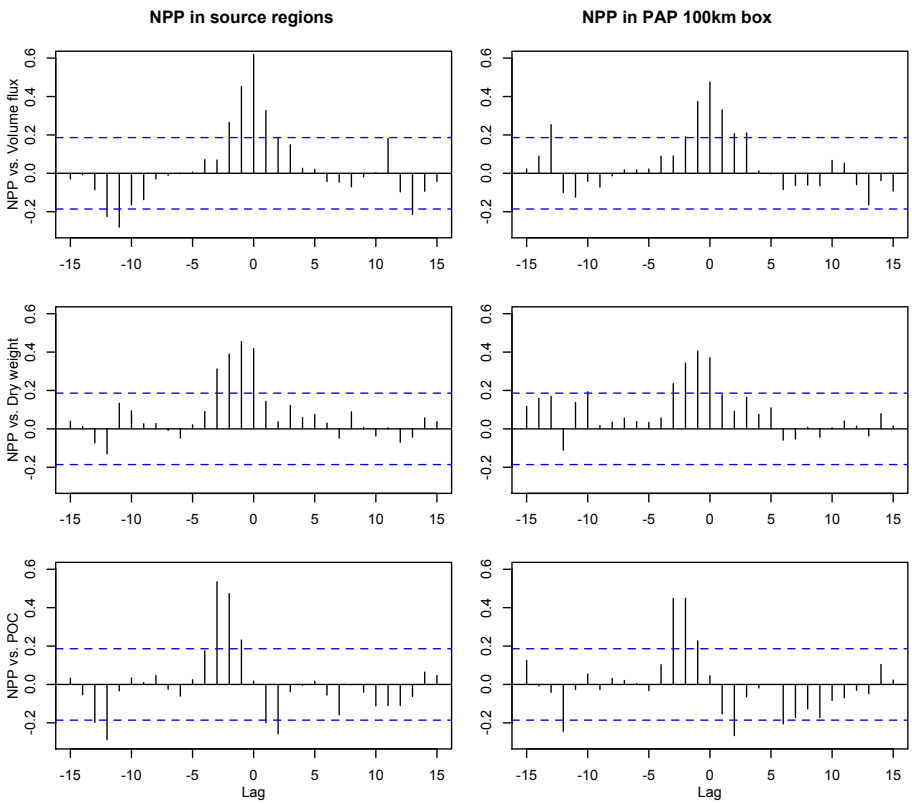

Figure 5. Cross-correlations between NPP in the source regions defined by particle tracking (left) or in a 100 km box around the PAP observatory (right) and sediment fluxes. The dashed lines show the 95 % confidence intervals. The unit of the lags is months.

BGD
12, 5169–5199, 2015